2009 IEEE International Conference on Robotics and Automation
Kobe International Conference Center
Kobe, Japan, May 12-17, 2009

Aerodynamics and Control of Autonomous Quadrotor Helicopters in Aggressive Maneuvering

Haomiao Huang
Stanford University
Stanford, California, 94305

Gabriel M. Hoffmann
Stanford University
Stanford, California, 94305

Steven L. Waslander
University of Waterloo
Waterloo, ON, Canada, N2L 3G1

Claire J. Tomlin
University of California
Berkeley, California, 94720

***Abstract*— Quadrotor helicopters have become increasingly important in recent years as platforms for both research and commercial unmanned aerial vehicle applications. This paper extends previous work on several important aerodynamic effects impacting quadrotor flight in regimes beyond nominal hover conditions. The implications of these effects on quadrotor performance are investigated and control techniques are presented that compensate for them accordingly. The analysis and control systems are validated on the Stanford Testbed of Autonomous Rotorcraft for Multi-Agent Control quadrotor helicopter testbed by performing the quadrotor equivalent of the stall turn aerobatic maneuver. Flight results demonstrate the accuracy of the aerodynamic models and improved control performance with the proposed control schemes.**

I. INTRODUCTION

Quadrotor helicopters have become increasingly popular as unmanned aerial vehicle (UAV) platforms. These vehicles have 4 identical rotors in 2 pairs spinning in opposite directions, and possess many advantages over standard helicopters in terms of safety and efficiency at small sizes. Several radio controlled toys have been constructed based on quadrotor planforms [1], [2], and many research groups have begun constructing quadrotor UAVs as robotics research tools [1], [3], [4], [5], [6], [7], [8], [9]. Several other groups are also developing quadrotor helicopters as general-use UAVs [10], [11].

Several groups have demonstrated controlled indoor position controlled flight, such as the OS4 quadrotor project [4], the MIT SWARM project [16], and a project using a controller proven to be globally stable [17]. In these previous projects, control algorithm designs used simplified dynamics, neglecting vehicle aerodynamics. Since many previous autonomous quadrotor projects have flown indoors, relatively little attention has been paid to the aerodynamics of quadrotors in conditions other than hovering and flying at low speeds.

Recent work has shown that at higher speeds and in outdoor flight several aerodynamic effects impact the flight characteristics of quadrotors. The Mesicopter project studied some first-order aerodynamic effects [18], while another group considered the effects of drag and thrust power under hover conditions [19]. The X-4 Flyer project at the Australian National University considered the effects of blade flapping and attitude damping from rotor ascent/descent rates [9]. The Stanford Testbed of Autonomous Rotorcraft for Multi-Agent Control (STARMAC) is one of the first successful quadrotor research platforms. Previous work with the STARMAC quadrotors has been among the first to address the issues of increasing flight speeds of quadrotors, and analyzed blade flapping and total thrust variation as two major aerodynamic influences on quadrotor aerodynamics [20], [21]. Static tests on a fixed thrust stand were used to compare measured data with analytical results, and flight tests were conducted to verify the presence and magnitude of these effects.

Fig. 1. The STARMAC II autonomous quadrotor helicopter in flight.

The work presented here takes the analysis of blade flapping and thrust variation and applies them to the creation of models and control techniques for operating a quadrotor at high speeds and under aggressive maneuvers. Simulations of a quadrotor are performed including these effects and validated against actual flights on the STARMAC quadrotors. A novel feedback linearization controller is presented which successfully compensates for these aerodynamic effects. This is the first time such control techniques have been applied to quadrotor helicopters.

This paper is structured as follows. Section II describes the STARMAC quadrotor helicopters used in the flight tests. The aerodynamic effects investigated in these experiments are described in Section III, and the existing STARMAC control system and the augmented system to reject aerodynamic disturbances are presented in Section IV. Simulation and experimental results are presented in Section V, followed by conclusions and future work.

Haomiao Huang is a PhD Candidate in Aeronautics and Astronautics. email: haomiao@stanford.edu

Gabriel Hoffmann is a Post-Doctoral Scholar in Aeronautics and Astronautics. email: hoffmann@stanford.edu

Steven L. Waslander is an Assistant Professor in the Department of Mechanical and Mechatronics Engineering at the University of Waterloo. email: stevenw@uwaterloo.ca

Claire J. Tomlin is a Professor in Electrical Engineering and Computer Sciences. email: tomlin@eecs.berkeley.edu

II. The STARMAC Testbed

STARMAC has been developed as an easy-to-use and reconfigurable platform for research in multi-vehicle control and path-planning, and has been used to demonstrate a variety of in such algorithms in autonomous outdoor flight. Recently, STARMAC was used to demonstrate a decentralized collision avoidance algorithm [12], cooperative search for rescue beacon tracking using a decentralized information theoretic control algorithm to coordinate aircraft [13], and path-planning and trajectory following in obstacle-rich environments [14], [15]. In each case, the flexibility and convenience of the quadrotor design have enabled rapid evaluation of new technologies.

The STARMAC quadrotors are custom-built vehicles 0.75 m on each side, weighing 1.1 kg to 1.5 kg depending on the computing configuration, with an additional payload capacity of roughly 1 kg. Each aircraft is equipped with an onboard 6-axis inertial measurement unit (IMU) and GPS receiver. Position and velocity are calculated at 10 Hz using carrier-phase differential GPS relative to a stationary base-station, giving accuracy of 2 cm in the horizontal plane. GPS position measurements are fused with IMU attitude rate and accelerometer measurements using an onboard Extended Kalman Filter (EKF). Local altitude sensing and control is achieved using an ultrasonic rangefinder.

Closed-loop attitude and altitude control are performed at 76 Hz using an Atmel Atmega128 microprocessor. The EKF and higher level planning and control are performed on either a Gumstix Verdex single board computer running embedded Linux, or for more complex sensor processing and onboard optimization, an Advanced Digital Logic PC104 running Fedora Linux. The PC104 is a dual-core 2 GHz processor with 1 GB of RAM, capable of performing many high level computing tasks.

The STARMAC quadrotors have proven to be a capable and useful flight test platform for many different applications. They are small and agile, yet capable of carrying a useful computing and sensing payload. A Hokuyo laser range finder, Videre stereo vision camera system, and Tracker DTS digital avalanche rescue beacon have been successfully flown on the aircraft [22], [23], [24].

III. Aerodynamic Effects

The two main aerodynamic effects addressed here are blade flapping and total thrust variation in translational flight. Blade flapping has a substantial effect on attitude control, while total thrust variation affects the thrust generated by the vehicle's rotors, thus having a large impact on altitude control. Both effects will be discussed here in sufficient detail as to understand their impact on the vehicle's flight characteristics.

A. Blade Flapping

A rotor in translational flight undergoes an effect known as blade flapping. The advancing blade of the rotor has a higher velocity relative to the free-stream, while the retreating blade sees a lower effective airspeed. This causes an imbalance

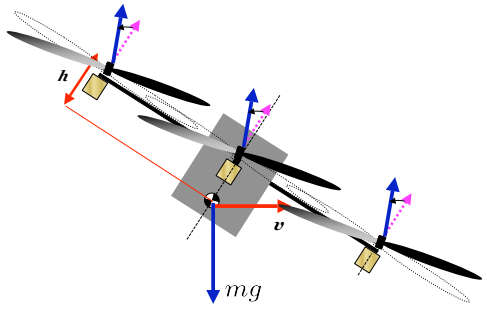

Fig. 2. Effect of blade flapping in forward flight: the deflection of the rotor plane due to flapping causes an effective deflection of the thrust vector, generating moments about the center of gravity.

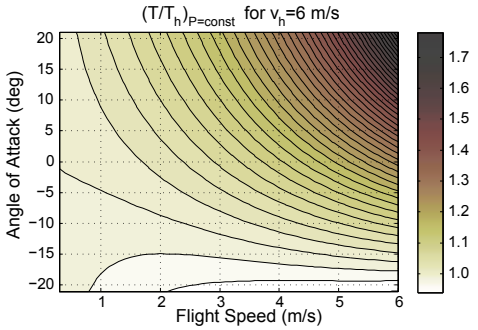

Fig. 3. Thrust dependence on angle of attack and vehicle speed for a constant power input. [21]

in lift, inducing an up and down oscillation of the rotor blades [25]. In steady state, this causes the effective rotor plane to tilt at some angle off of vertical, causing a deflection of the thrust vector (see Figure 2). If the rotor plane is not aligned with the vehicle's center of gravity, this will create a moment about the center of gravity (c.g.) that can degrade attitude controller performance [9]. For stiff rotors without hinges at the hub, there is also a moment generated directly at the rotor hub from the deflection of the blades.

The full analysis of blade flapping is beyond the scope of this paper, but is presented in more detail in the helicopter literature and in previous work [25], [26], [21]. Due to the quadrotor's bilateral symmetries, moments generated by lateral deflections of the rotor plane cancel. The backward tilt of the rotor plane through a deflection angle a_{1s} generates a longitudinal thrust, causing a moment

$$M_{b,lon} = Th \sin a_{1s} \tag{1}$$

where h is the vertical distance from the rotor plane to the c.g. of the vehicle and T is the thrust. The moment at the rotor hub from the bending of the blades is

$$M_{b,s} = k_\beta a_{1s} \tag{2}$$

where k_β is the stiffness of the rotor blade in Nm/rad. The total longitudinal moment created by blade flapping M_{bf} is the sum of these two moments.

B. Total Thrust Variation in Translational Flight

Total thrust variation encompasses two related effects: effective translational lift and a change in thrust due to angle of attack. As a rotor moves translationally, the relative momentum of the airstream causes an increase in lift. This is known as translational lift. The angle of attack (AOA) of the rotor with respect to the free-stream also changes the lift, with an increase in AOA increasing thrust, as in aircraft wings. The analysis of these effects are explored in more depth in the helicopter literature [27], [25] and in prior work [21], and simply summarized here.

A rotor generates thrust by inducing a velocity on the air that passes through it. At hover thrust T_h, the induced velocity v_h is derived from momentum analysis as

$$v_h = \sqrt{\frac{T_h}{2\rho A}} \tag{3}$$

where A is the area swept out by the rotor blades and ρ is the density of air. This can be related to the induced velocity in translational flight v_i (for an ideal vehicle) as [27]

$$v_i = \frac{v_h^2}{\sqrt{(v_\infty \cos\alpha)^2 + (v_i - v_\infty \sin\alpha)^2}} \tag{4}$$

where α is the angle of attack of the rotor plane with respect to a free stream flow with velocity v_∞, with the convention that positive values correspond to pitching up (as with airfoils). Using this expression for v_i, the ideal thrust T for a given power input P can be computed as

$$T = \frac{P}{v_i - v_\infty \sin\alpha} \tag{5}$$

where the denominator in Equation (5) is the air speed across the rotors. The power input required for a nominal thrust at hover P_h can be calculated as

$$P_h = \frac{T_h^{3/2}}{\sqrt{2\rho A}} \tag{6}$$

Combining these equations allows a ratio to be calculated between the actual thrust produced in translational flight and the nominal thrust at hover produced for a given motor command (Figure 3).

IV. Control Implementation

Control of quadrotor helicopters is achieved by varying the thrust of two sets of counter-rotating rotor pairs. Altitude is controlled with the total thrust of all rotors, and lateral acceleration is controlled through the pitch and roll of the aircraft. Attitude is controlled through differential actuation of opposing rotors, with yaw controlled using the difference in reaction torques between the pitch and roll rotor pairs. This section will discuss the inertial dynamics of the quadrotor, the existing attitude and altitude control scheme on STARMAC, and present the adjustments made to compensate for the aerodynamic effects discussed above.

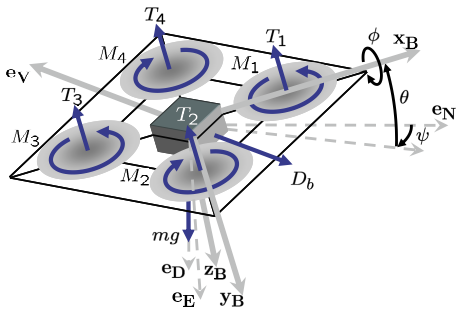

Fig. 4. Free body diagram showing forces and moments on a quadrotor helicopter relative to both the body and inertial frames of reference.

A. Inertial Dynamics

The thrust produced by the j^{th} rotor acts perpendicularly to the rotor plane along the $\mathbf{z}_{R_j}$ axis, which defines the axis of the rotor relative to the vehicle (note that this may change in flight). The vehicle body drag force is $D_b \propto v_\infty^2$, vehicle mass is m, acceleration due to gravity is g, and the inertia matrix is $I_B \in \mathbb{R}^{3\times3}$. A free body diagram is depicted in Figure 4.

The total force $\mathbf{F}$ on the vehicle is

$$\mathbf{F} = -D_b \mathbf{e}_v + mg\mathbf{e}_D + \sum_{j=1}^{4} \left(-T_j R_{R_j,I} \mathbf{z}_{R_j}\right) \tag{7}$$

where $R_{R_j,I}$ is the rotation matrix from the plane of rotor j to inertial coordinates and $\mathbf{e}_v$ and $\mathbf{e}_D$ are the body velocity and down directions. The total moment on the vehicle $\mathbf{M}$, is

$$\mathbf{M} = \sum_{j=1}^{4} \left(\mathbf{M}_j + \mathbf{M}_{bf,j} + \mathbf{r}_j \times \left(-T_j R_{R_j,B} \mathbf{z}_{R_j}\right)\right) \tag{8}$$

where $R_{R_j,B}$ is the rotation matrix from the plane of rotor j to body coordinates and $\mathbf{r}_j$ is the vector from the c.g. to each rotor. $\mathbf{M}_j$ and $\mathbf{M}_{bf,j}$ are the reaction torque and flapping moment from each rotor, respectively. The moment due to aerodynamic drag is neglected. The full nonlinear dynamics including angular rates ω_B can be described as,

$$\mathbf{F} = m\ddot{\mathbf{x}} \tag{9}$$

$$\mathbf{M} = I_B\dot{\omega}_B + \omega_B \times I_B\omega_B \tag{10}$$

where the total angular momentum of the rotors is assumed to be near zero, as the momentum from the counter-rotating pairs cancels when yaw is held steady.

B. Attitude and Altitude Control

Within the STARMAC vehicle's operational range (attitudes within $\pm30°$), the equations of motion are approximately decoupled about each attitude axis. STARMAC uses a 3-2-1 Euler angle rotation of roll ϕ, pitch θ, and yaw ψ. The control input thrusts about each axis, u_ϕ, u_θ, and u_ψ, are implemented independently as differential commands to motor pairs. The inputs for each motor are added to the

total thrust control input u_z to generate thrust commands u_1 through u_4, for motors 1 through 4,

$$\begin{aligned} u_1 &= -u_\theta + u_\psi + u_z \\ u_2 &= u_\phi - u_\psi + u_z \\ u_3 &= u_\theta + u_\psi + u_z \\ u_4 &= -u_\phi - u_\psi + u_z \end{aligned} \tag{11}$$

Attitude control is implemented using a standard Porportional-Integral-Derivative (PID) controller augmented with feedback on angular acceleration, resulting in the following control law for roll:

$$u_\phi = k_{dd}(\ddot{\phi}_{ref} - \ddot{\phi}) + k_d(\dot{\phi}_{ref} - \dot{\phi}) + k_p(\phi_{ref} - \phi) + k_i \int_0^t (\phi_{ref} - \phi)dt \tag{12}$$

where k_{dd}, k_d, k_p, and k_i are the double derivative (angular acceleration), derivative, proportional, and integral control gains respectively. ϕ_{ref} is the commanded reference roll. Controls for pitch and yaw are implemented similarly.

Altitude control is also implemented using a PID controller augmented with feedback on acceleration, with feedback linearization to compensate for the force of gravity when rolling and pitching. The resulting control law is:

$$u_z = \frac{1}{\cos\phi\cos\theta}(k_{dd,alt}(\ddot{z}_{ref} - \ddot{z}) + k_{d,alt}(\dot{z}_{ref} - \dot{z}) + k_{p,alt}(z_{ref} - z) + T_{nom}) \tag{13}$$

where z is the altitude and z_{ref} is the reference command. T_{nom} is the nominal offset thrust required to overcome the force of gravity.

These controllers, hence referred to as the default controller scheme, have been demonstrated to have very good tracking performance near hover and when subjected to suddenly varying attitude commands at low velocities [21]. Typical RMS errors at speeds on the order of 3 m/s or less are approximately 0.65° in attitude and 0.02 m in altitude.

C. Compensating for Aerodynamics

The default controller is able to successfully reject small disturbances, steady-state larger disturbances, and some model error, but not the type of disturbances associated with the aerodynamic effects discussed above. To compensate for these, the disturbance forces and moments are calculated using the vehicle state and feedback linearization is used to cancel out both flapping moments and translational thrust effects. The flap angle is modeled using a linear approximation, where compensating moments are calculated assuming decoupling of the body axes. The flap angle in each body axis calculated as

$$a_{1s,x} = k_f v_{b,x} \tag{14}$$

where $v_{b,x}$ is the velocity in the body x axis and $a_{1s,x}$ is the flap angle along the x axis. k_f is an experimentally measured constant relating flapping to wind velocity, found to be about $0.009\frac{rads}{m}$, resulting in flapping angles of up to 5° at 10 m/s. The blade stiffness k_β was also measured experimentally. The corresponding moment M_θ about the pitch axis required to compensate is then

$$M_\theta = -4(k_\beta a_{1s,x} + Th\sin a_{1s,x}) \approx -4(k_\beta + Th)a_{1s,x} \tag{15}$$

and a similar compensating moment is calculated for the roll axis.

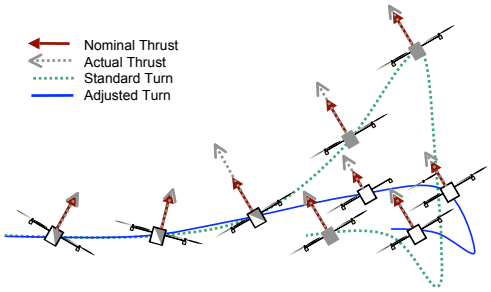

Fig. 5. The standard stall turn maneuver uses the extra thrust generated by a sudden increase in angle of attack to quickly reverse the aircraft's direction. Decreasing commanded thrust to compensate results in a flatter trajectory.

Thrust compensation is achieved using Equations (4) and (5). Due to the need to find roots of a quartic equation to solve for v_i in Equation (4), a lookup table is used for computational efficiency. Using Equation (5), the actual thrust T produced at a given AOA and velocity relative to the nominal hover thrust T_h can be calculated as

$$\frac{T}{T_h} = \frac{v_h}{v_i - v_\infty \sin\alpha} \tag{16}$$

This allows a table to be built up giving the hover thrust T_h required to achieve a desired actual thrust T. The desired thrust is calculated by the altitude and attitude controllers normally, and the table is used to find the thrust T_h to be commanded in order to generate that desired thrust.

V. Experimental Results

To validate the analysis and controller design presented above, a series of flights were conducted on the STARMAC quadrotor demonstrating both the influence of the aerodynamics and the success of the controller design at rejecting those disturbances. The influence of blade flapping and total thrust variation were explored using a maneuver known as the stall turn. This is the first time these effects have been demonstrated and compensated for in a quadrotor testbed.

A. The Stall Turn

The stall turn is an aerobatic maneuver first developed by fighter pilots as a means of rapidly changing direction [28]. A sudden pitch moment is applied in level flight, rapidly increasing the angle of attack and increasing the lift force generated by the wings. The aircraft pops into a steep climb, trading kinetic energy for height. At the peak of the climb velocity is low, and a yaw moment is applied to reverse direction. The maneuver is carried out in a similar fashion with helicopters. Due to the symmetry of a quadrotor configuration, no change in yaw is needed to reverse direction; for the quadrotor a stall turn consists of high-speed forward

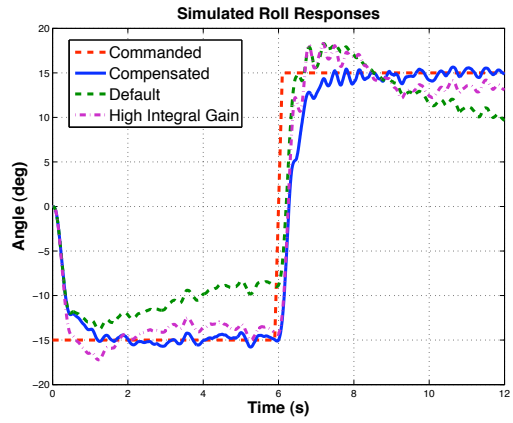

(a)

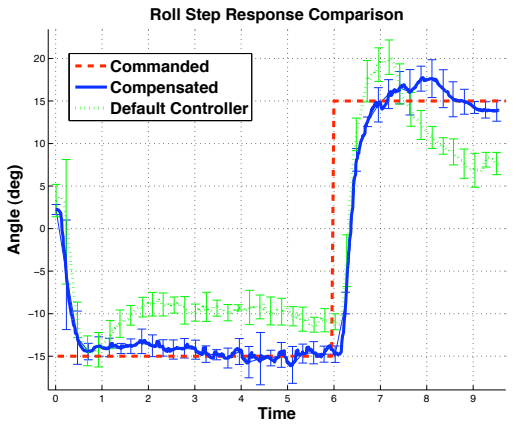

(b)

Fig. 6. (a) Simulated response of the default, flapping compensated, and high integral gain controllers to roll commands. (b) Actual flight response of the default and flapping compensated controllers over a series of flights.

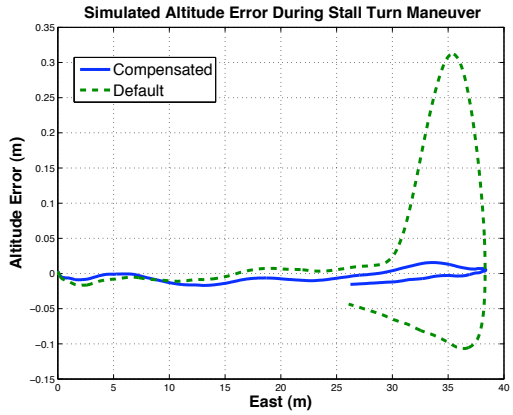

(a)

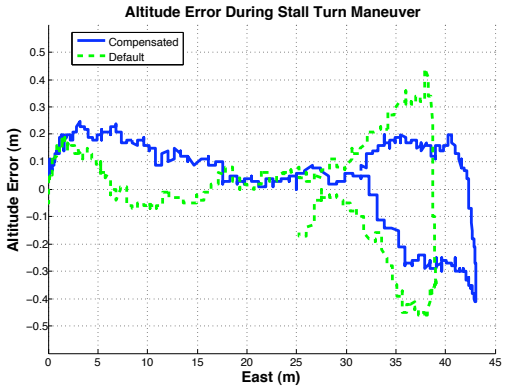

(b)

Fig. 7. (a) Simulated response of the default and vertically compensated controllers in a stall turn. (b) Actual flight response of the default and compensated controllers in a single flights.

flight followed by a reversal of attitude command. This is a situation that may often be encountered in autonomous flight, for example due to the need to avoid some obstacle that suddenly comes into view.

The stall turn is an excellent way to demonstrate both blade flapping and thrust variation. These turns are carried out at fairly high speeds (roughly $8m/s$). The sustained attitude angle and high translational speed required to enter the maneuver cause significant blade flapping moments that must be compensated for. The sudden change in angle-of-attack causes a large increase in thrust, as predicted by the analysis presented in Section III. The vertical compensation control presented above can cancel the sudden thrust increase, resulting in a much flatter trajectory (see Figure 5).

B. Results

To validate the analysis presented above, a STARMAC quadrotor executed a series of open-loop stall turn maneuvers. The controller compensation for blade flapping and total thrust variation were tested separately. Results for blade flapping are presented in Figure 6, and results for thrust variation are presented in Figure 7. Experimental results are compared against a nonlinear 6-DOF simulator of the quadrotor's dynamics incorporating the aerodynamic effects.

Figure 6 shows the response of the aircraft to the initial command in roll necessary to build up speed for the stall turn. Simulation results are shown for the default, flapping compensated, and high integral gain attitude controllers, and flight results are shown for the default and compensated controllers. The figure shows results averaged over 6 flights each with the default and compensated controllers.

The simulated results match well with actual flight data, validating the models used. Without the feedback compensation for the moments generated by blade flapping, the default controller is unable to sustain the large commanded pitch, resulting in sustained tracking errors of up to 5°. Since the velocity is increasing, the flapping moment is also continuously increasing more quickly than the integrator can compensate for. A controller was also simulated with a much larger integral gain, which is better able to reject the flapping moments but results in increased overshoot. Flight results for the large integral gain controller are not shown here due to the fact that previous controller experiments with large integral gain on the attitude control showed instability and large overshoots even under nominal flying conditions. The compensated controller is able to successfully track the sustained commanded roll and transition to the following

command with less overshoot. The linear control loop is also able to protect against model and sensor uncertainties associated with the feedback linearization.

Compensating for the increase in thrust due to changes in angle of attack results in improved altitude tracking performance during sudden changes in attitude, as shown in Figure 7. By decreasing thrust appropriately during the stall turn maneuver, the reversal in direction is accomplished without a large increase in altitude. The flight results show a large drop in altitude at the end of the maneuver in either case due to an error in the acceleration term of the controller, in which the body acceleration instead of the inertial acceleration. This has since been corrected and shown to have no effect on the pop-up, and full flight tests using the compensated controller are in progress.

VI. CONCLUSIONS AND FUTURE WORKS

The quadrotor helicopter has proven to be a useful autonomous platform, and for high-speed flights outside the hover regime it is important to understand and account for the aerodynamics of the vehicle. The results presented in this paper have demonstrated several aerodynamic effects that quadrotors are subject to, and that disturbances arising from these effects can be successfully rejected using the appropriate controllers.

Future work extends in several directions. First, further investigation into the aerodynamics of the quadrotor will be pursued. The light weight and low thrusts of the quadrotor means that at higher speeds the vehicle may encounter effects such as vortex ring state at low angles of attack, which will greatly affect the control of the vehicle. Also, the controllers presented here have been designed towards minimizing the impact of the aerodynamic effects, making the quadrotors more like the linear plants assumed by previous path-planning software. Another approach is to design path planning algorithms which take advantage of the aerodynamic effects to enable highly aggressive aerobatic trajectories. A better understanding of the high-speed aerobatics will enable such flights, as well as allowing analysis to verify safety and performance bounds during these maneuvers.

ACKNOWLEDGMENTS

The authors would like to thank Michael Vitus , Jeremy Gillula, and Vijay Pradeep for their assistance on the STARMAC project and in flight testing.

REFERENCES

[1] E. Altuğ, J. P. Ostrowski, and C. J. Taylor, "Quadrotor control using dual camera visual feedback," in *Proceedings of the IEEE International Conference on Robotics and Automation*, (Taipei, Taiwan), pp. 4294–4299, Sept 2003.

[2] DraganFly-Innovations, *DraganFlyer IV*. 2006. `http://www.rctoys.com`.

[3] G. Hoffmann, D. G. Rajnarayan, S. L. Waslander, D. Dostal, J. S. Jang, and C. J. Tomlin, "The stanford testbed of autonomous rotorcraft for multi agent control (STARMAC)," in *Proceedings of the 23rd Digital Avionics Systems Conference*, (Salt Lake City, UT), pp. 12.E.4/1–10, November 2004.

[4] S. Bouabdallah, P. Murrieri, and R. Siegwart, "Towards autonomous indoor micro VTOL," *Autonomous Robots*, vol. 18, pp. 171–183, March 2005.

[5] N. Guenard, T. Hamel, and V. Moreau, "Dynamic modeling and intuitive control strategy for an x4-flyer," in *Proceedings of the International Conference on Control and Automation*, (Budapest, Hungary), pp. 141–146, June 2005.

[6] J. Escareño, S. Salazar-Cruz, and R. Lozano, "Embedded control of a four-rotor UAV," in *Proceedings of the AACC American Control Conference*, (Minneapolis, MN), pp. 3936–3941, June 2006.

[7] E. B. Nice, "Design of a four rotor hovering vehicle," Master's thesis, Cornell University, 2004.

[8] S. Park *et al.*, "RIC (robust internal-loop compensator) based flight control of a quad-rotor type UAV," in *Proceedings of the IEEE/RSJ International Conference on Intelligent Robotics and Systems*, (Edmonton, Alberta), August 2005.

[9] P. Pounds, R. Mahony, and P. Corke, "Modeling and control of a quad-rotor robot," in *Proceedings of the Australasian Conference on Robotics and Automation*, (Auckland, New Zealand), 2006.

[10] S. Craciunas, C. Kirsch, H. Rock, and R. Trummer, "The javiator: A high-payload quadrotor UAV with high-level programming capabilities," in *Proceedings of the 2008 AIAA Guidance, Navigation, and Control Conference*, (Honolulu, Hawaii), 2008.

[11] Ascending Technologies, *Multi-Rotor Air Vehicles*. `http://www.asctec.de/`.

[12] S. L. Waslander, G. Inalhan, and C. J. Tomlin, "Decentralized optimization via nash bargaining," in *Theory and Algorithms for Cooperative Systems* (D. Grundel, R. Murphey, and P. M. Pardalos, eds.), vol. 4, pp. 565–585, World Scientific Publishing Co., 2004.

[13] G. M. Hoffmann and C. J. Tomlin, "Mobile sensor network control using mutual information methods and particle filters," *in review for IEEE Transactions on Automatic Control*, 2008.

[14] M. P. Vitus, V. Pradeep, G. Hoffmann, S. L. Waslander, and C. J. Tomlin, "Tunnel-MILP: Path planning with sequential convex polytopes," in *In the Proceedings of the AIAA Guidance, Navigation, and Control Conference*, (Honolulu, Hawaii, USA), 2008.

[15] G. M. Hoffmann, S. L. Waslander, and C. J. Tomlin, "Flight test and simulation results for an autonomous aerobatic helicopter," in *Proceedings of the 2008 AIAA Guidance, Navigation, and Control Conference*, (Honolulu, Hawaii), 2008.

[16] M. Valenti, B. Bethke, G. Fiore, J. P. How, and E. Feron, "Indoor multi-vehicle flight testbed for fault detection, isolation, and recovery," in *Proceedings of the AIAA Guidance, Navigation and Control Conference and Exhibit*, (Keystone, CO), August 2006.

[17] S. Salazar-Cruz, S. Palomino, and R. Lozano, "Trajectory tracking for a four rotor mini-aircraft," in *Proceedings of the 44th IEEE Conference on Decision and Control*, (Seville, Spain), pp. 2505–2510, December 2005.

[18] I. Kroo, F. Prinz, M. Shantz, P. Kunz, G. Fay, S. Cheng, T. Fabian, and C. Partridge, "The mesicopter: A miniature rotorcraft concept, phase ii interim report," 2000.

[19] A. Mokhtari and A. Benallegue, "Dynamic feedback controller of euler angles and wind parameters estimation for a quadrotor unmanned aerial vehicle," in *Proceedings of the 2004 IEEE Conference on Robotics & Automation*, (New Orleans, LA), 2004.

[20] G. M. Hoffmann, H. Huang, S. L. Waslander, and C. J. Tomlin, "Quadrotor helicopter flight dynamics and control: Theory and experiment," in *Proceedings of the AIAA Guidance, Navigation, and Control Conference and Exhibit*, (Hilton Head, SC), August 2007.

[21] G. Hoffmann, S. L. Waslander, H. Huang, and C. J. Tomlin, "Autonomous quadrotor helicopter testbed design, control, and experiments," *AIAA Journal of Guidance, Control, and Dynamics*. Submitted.

[22] Hokuyo, *URG-04LX Laser Range Finder*. `http://www.hokuyo-aut.jp/products/urg/urg.htm`.

[23] Videre Design, *STH-MDCS 2 Stereo Vision Head*. `http://www.videredesign.com/sthmdcs2.htm`.

[24] BackCountry Access, *Tracker DTS Digital Avalanche Beacon*. `http://www.bcaccess.com/bca\_products/tracker/index.php`.

[25] R. W. Prouty, *Helicopter Performance, Stability, and Control*, pp. 143–146, 476–477. Malabar, FL: Krieger Publishing Company, 1990.

[26] S. Newman, *The Foundations of Helicopter Flight*, pp. 107–116. New York, NY: Halsted Press, 1994.

[27] J. G. Leishman, *Principles of Helicopter Aerodynamics*, pp. 36–71. New York, NY: Cambridge University Press, 2000.

[28] R. L. Shaw, *Fighter Combat - Tactics and Maneuvering*. Annapolis, Maryland: Naval Institute Press, 1985.